Pei *et al. Chem. Synth.* **2025**, *5*, 47
DOI: 10.20517/cs.2024.181

Chemical Synthesis

Mini Review

Open Access

Check for updates

Alloyed single-atom catalysts for electro- and photo-catalytic water splitting

Guang-Xian Pei[1,2,*], Haifeng Qi[3], Jan Philipp Hofmann[4]

[1]Qingdao Institute of Bioenergy and Bioprocess Technology, Chinese Academy of Sciences, Qingdao 266101, Shandong, China.
[2]Shandong Energy Institute, Qingdao 266101, Shandong, China.
[3]Max Planck-Cardiff Centre on the Fundamentals of Heterogeneous Catalysis FUNCAT, Translational Research Hub, Cardiff University, Cardiff CF24 4HQ, UK.
[4]Surface Science Laboratory, Department of Materials- and Geosciences, Technical University of Darmstadt, Darmstadt 64287, Germany.

[*]**Correspondence to:** Prof. Guang-Xian Pei, Qingdao Institute of Bioenergy and Bioprocess Technology, Chinese Academy of Sciences, Songling Road No. 189, Qingdao 266101, Shandong, China. E-mail: peigx@qibebt.ac.cn

How to cite this article: Pei, G. X.; Qi, H.; Hofmann, J. P. Alloyed single-atom catalysts for electro- and photo- catalytic water splitting. *Chem. Synth.* **2025**, *5*, 47. https://dx.doi.org/10.20517/cs.2024.181

Received: 18 Nov 2024 **First Decision:** 18 Dec 2024 **Revised:** 14 Jan 2025 **Accepted:** 6 Feb 2025 **Published:** 13 May 2025

Academic Editors: Feng Shi, Jun Xu **Copy Editor:** Pei-Yun Wang **Production Editor:** Pei-Yun Wang

Abstract

Water splitting by using renewable energy to produce hydrogen and oxygen can be regarded as one of the most promising approaches for sustainable energy conversion. Developing cost-effective and high-performance water splitting catalysts plays an increasingly important role in enhancing overall efficiency. Alloyed single-atom catalysts (alloyed SACs, also known as single-atom alloy), with one of the metal atoms atomically dispersed in a host metal, combine the advantages of both SACs and traditional metal alloys. They show the maximum utilization of active metal atoms and uniquely geometric and electronic structures, offering great potential in reducing the cost of catalyst and boosting the performance in catalytic water splitting. This review aims to provide a comprehensive summary of the development of alloyed SACs for oxygen and hydrogen evolution reactions by water splitting. We start with a brief introduction of the mechanism for water splitting under electrocatalytic and photocatalytic conditions, followed by emphasizing the merits of the formation of alloyed SACs for water splitting. Then, the case studies of electro- and photo- catalytic hydrogen and oxygen evolution via water splitting are illustrated and discussed. Finally, challenges and prospects are provided, with further continued efforts expected for achieving future exciting progress in tailoring the active sites for designing high-performance catalysts.

Keywords: Alloyed single-atom catalyst, photocatalysis, electrocatalysis, water splitting, oxygen evolution reaction, hydrogen evolution reaction

INTRODUCTION

Water splitting using renewable energy to produce hydrogen and oxygen has been recognized as one of the most promising ways to store energy for future chemical transformation[1,2]. To realize the reaction with high energy efficiency, design and synthesis of high-performance water splitting catalysts are important. The strategies for optimizing catalysts both economically and efficiently include increasing the intrinsic reactivity of the metal atoms, optimizing the exposure of the active sites, constructing synergy effects with multiple metal elements and so forth. For instance, single-atom catalysts (SACs), with their maximum utilization of the metal active sites at the atomic level, have been extensively studied for water splitting, while the poor stability significantly limits their practical utilization[3]. Alloying strategies have long been recognized as a promising approach to enhance catalytic performance by rationally designing the electronic structures, arranging atomic configurations and optimizing the synergy effect of different metal elements[4,5]. For example, compared with their monometallic counterparts, Pt-Zn[6], Pt-Ni[7], and Pd-Ir[8] alloy nanocatalysts have been proved to demonstrate superior catalytic performance for water splitting to produce hydrogen and oxygen. Nevertheless, due to the random distribution of the metal atoms, the utilization of the active sites is insufficient.

The formation of alloyed SACs, in which the catalytically active metal atoms are atomically isolated by another metal element, can make use of the active metal element at the atomic level, and the catalytic performance will be further optimized due to the synergy effect between different metal elements. Thus, since the first demonstration of the isolated Pd atoms on Cu(111) for semi-hydrogenation of alkynes[9], such catalysts have been extensively investigated for various catalytic applications, including oxidation, dehydrogenation, photocatalysis, electrocatalysis and so forth[10-13]. Our previous work also demonstrated that group IB metals (Au, Ag and Cu) alloyed Pd SACs displayed excellent catalytic performance for acetylene semi-hydrogenation under simulated industrial conditions[14-17]. Recently, increasing attention has been paid to the catalytic applications of alloyed SACs for sustainable energy conversion[18-22]. For instance, the core/shell nanocrystals of densely packed Cu/CuAu material with intermetallic alloyed single atom layer structure demonstrated excellent selectivity toward NH_3 for the electrocatalytic nitrate reduction reaction[23]. The enhanced catalytic performance has been ascribed to the formation of alloyed Au single atoms into the Cu matrix, which can introduce ligand effects and thus optimize the $^*NO_3$ and $^*N$ chemisorption. Similarly, single-atom Bi-decorated Cu also demonstrated remarkably enhanced C_2^+ product selectivity for CO_2 electrocatalytic reduction[24], with an optimal Faradaic efficiency (FE) of 73.4%, which was superior to that of the pure Cu or Bi nanoparticle-decorated Cu nanocomposites.

The synthesis, characterization, and varied catalytic applications of alloyed SACs have been summarized and discussed by several reviews[10-13,18-22], while there is still no summarized discussion on their catalytic application for water splitting. Herein, we first start with a brief introduction of the mechanism for water splitting via electrocatalytic and photocatalytic processes, followed by discussing the merits of alloyed SACs for water splitting; then, special attention is paid to the cases of electrocatalytic and photocatalytic hydrogen evolution and oxygen evolution by water splitting. Finally, challenges and outlooks are provided and discussed for guiding the rational design of highly efficient catalysts for water splitting.

FUNDAMENTALS FOR WATER SPLITTING

The overall chemical reaction for water splitting is expressed as:

$$2H_2O \rightarrow 2H_2 + O_2 \quad (1)$$

Water splitting for oxygen evolution reaction (OER) and hydrogen evolution reaction (HER) can theoretically be realized with a minimum voltage of 1.23 V at room temperature. However, normally, additional energy is needed to drive these reactions. For electrocatalysis, it is manifested as the potential bias exceeding the minimum of 1.23 V. While for photocatalysis, photoexcitation energies above 2 eV are required. We will briefly discuss these in this section.

Electrocatalytic water splitting

For acidic electrolytes, OER occurs at the anode, while the HER takes place at the cathode. The corresponding reactions are as follows:

$$2H_2O \rightarrow 4H^+ + O_2 + 4e^- \quad (2)$$

$$4e^- + 4H^+ \rightarrow 2H_2 \quad (3)$$

Under alkaline conditions, HER and OER can be expressed as:

$$4H_2O + 4e^- \rightarrow 4OH^- + 2H_2 \quad (4)$$

$$4OH^- \rightarrow O_2 + 2H_2O + 4e^- \quad (5)$$

The extra voltage needed for reaching specific current density is named overpotential (η). Catalysts are used to minimize η as much as possible. In alkaline solutions, transition metals and their alloys are usually used for HER[25]; transition metal oxides can function effectively for OER[26]. Under acidic conditions, precious metals and precious metal oxides are normally effective catalysts for water splitting, such as RuO_2 and IrO_2 at the anode and Pt at the cathode[27].

The detailed mechanism for HER and OER varies under different conditions. Herein, we will simply discuss the generally accepted mechanisms for HER. Two steps are involved for HER in alkaline and acidic media: electrochemical reaction and conversion step [Figure 1][28]. The electrochemical reaction step, also named Volmer reaction, undergoes the following reactions:

$$* + H^+ + e^- \rightarrow {}^*H \text{ (acidic)} \quad (6)$$

$$* + H_2O + e^- \rightarrow {}^*H + OH^- \text{ (alkaline)} \quad (7)$$

Here, $^*H$ represents H atoms adsorbed over the active sites and * denotes active centers over the catalyst. In terms of the conversion step, $^*H$ undergoes either recombination (Tafel reaction) or electrochemical desorption (Heyrovsky reaction) to generate H_2, which depends on the nature of the electrode material. For the Heyrovsky reaction, one of the solvated H_2O or H^+ from the water layer interacts with $^*H$ to generate H_2:

$$^*H + H^+ + e^- \rightarrow * + H_2 \text{ (acidic)} \quad (8)$$

$$^*H + H_2O + e^- \rightarrow * + OH^- + H_2 \text{ (alkaline)} \quad (9)$$

The Tafel step is completed via the following reaction to produce H_2, followed by H_2 desorption from the electrode surface:

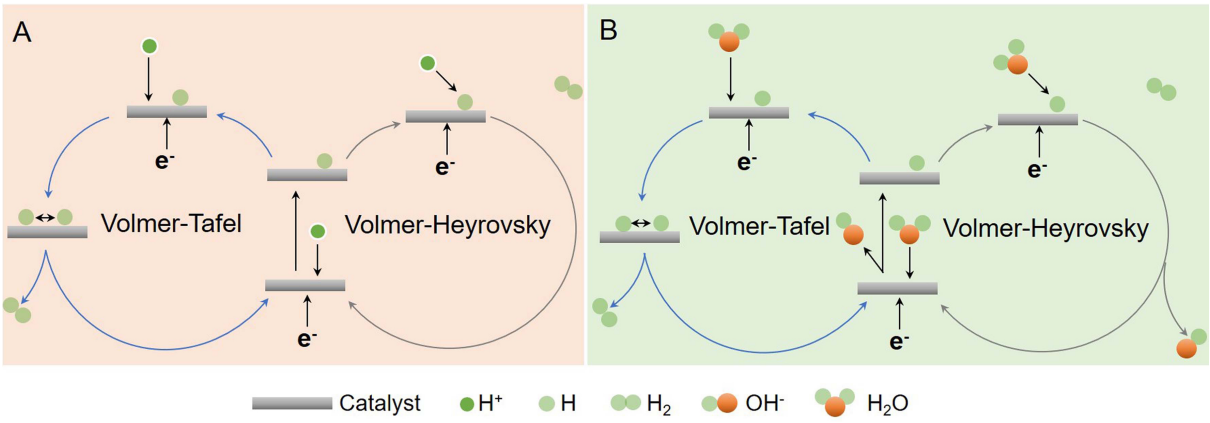

Figure 1. Mechanism for electrocatalytic HER in (A) acidic and (B) alkaline medium. HER: Hydrogen evolution reaction.

$$^{*}H + {}^{*}H \rightarrow 2^{*} + H_2 \quad (10)$$

Over decades of study, four main mechanisms are proposed for OER: lattice oxygen-mediated mechanism (LOM), adsorbate evolution mechanism (AEM), bi-nuclear mechanism (BNM), and oxide path mechanism (OPM)[1]. In this work, we will simply express the mechanism for OER in an acidic medium in

$$2H_2O - 4e^- \rightarrow 4H^+ + O_2 \quad (11)$$

when OER occurs in a neutral or alkaline solution, we employ

$$4OH^- - 4e^- \rightarrow 2H_2O + O_2 \quad (12)$$

with the possible elementary steps shown in Figure 2. According to the above explanation, OER involves a complex four-electron transfer process, which leads to significantly slower kinetics than HER. Thus, OER is both the thermodynamic and kinetic bottleneck for water splitting.

Photocatalytic water splitting

For photocatalysis, a semiconductor with a suitable bandgap is needed to absorb photon energy to drive the generation of electron-hole pairs; holes and electrons are generated in the valence and conduction bands, respectively. The hole and electron generated by photoexcitation drive water splitting to occur similarly to electrocatalysis [Figure 3][29]: with electrons reducing protons to produce H_2 and holes oxidizing water to produce O_2. Thus, a photocatalytic process can be divided into three steps[29]: (i) photons with energy higher than the bandgap values are absorbed to generate electron-hole pairs in a semiconductor; (ii) photogenerated charge migration and separation; and (iii) redox reactions at the surface.

However, though the generated holes and electrons are thermodynamically suitable for the reaction, electron-hole pairs will easily recombine if there are not enough active sites for driving transfer of holes and electrons for the reaction to occur[30]. Co-catalysts (e.g., Pt, RuO_2, and alloys) can be loaded onto the semiconductor surface to act as active sites for driving water splitting[30].

For both electrocatalytic and photocatalytic processes, catalysts play important roles. Normally, synergy effects between different metal elements are usually considered for enhancing catalytic efficiency.

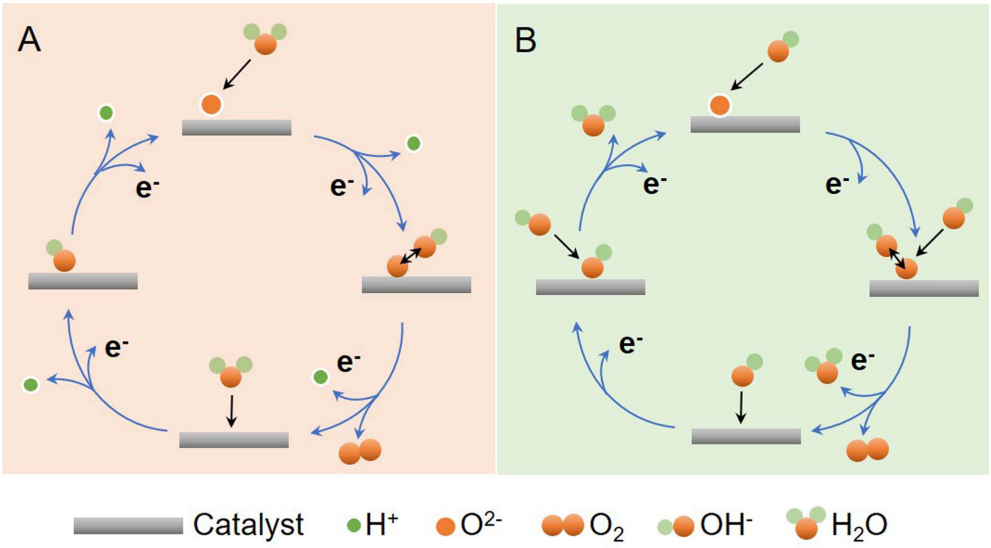

Figure 2. Mechanism for electrocatalytic OER in (A) acidic and (B) alkaline medium. OER: Oxygen evolution reaction.

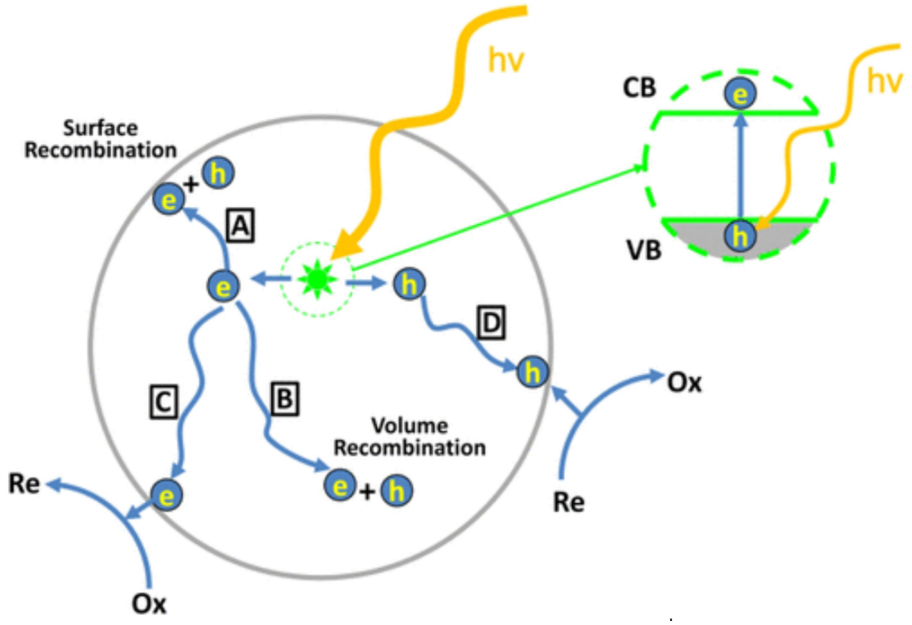

Figure 3. Schematic illustration of the photoexcitation in a semiconductor followed by deexcitation events. This figure is quoted with permission from ref[29]. Copyright 2012, American Chemical Society.

ADVANTAGES OF ALLOYED SACs FOR WATER SPLITTING

Catalytic stability

Atomic-level utilization of active sites is significantly important. SACs, which make use of active metal elements with atomic precision, have gained great attention in recent years. However, the stability of SACs under electrocatalytic conditions is poor which limits their utilization for water splitting and other electrocatalytic applications[3]. Different from most SACs, single atoms alloyed with other metal elements can significantly enhance stability. This is because, in one aspect, the ensembles are the thermodynamically preferred phase for many alloyed single atoms, and sintering of the isolated atom sites into ensembles can

be largely inhibited. Additionally, after forming an alloy with another metal element, the stability during photocatalysis or electrocatalysis processes can be largely enhanced due to the formation of nanoparticles/clusters. For instance, the performance and structure could be well maintained for the flow cell system at a current density of 400 $mA{\cdot}cm^{-2}$ for single-atom Bi-decorated Cu nanocomposites[24]. Furthermore, the oxidation of metallic catalysts can be largely suppressed under positive potential, thus demonstrating superior stability for electrocatalytic OER. For instance, the electrocatalytic stability for OER over Ru_1-Pt_3Cu was greater than that of RuO_2[31]. This illustrated that after the formation of alloyed single atoms, the stability limitation of the catalysts is the stability of the nanoparticles/clusters rather than the isolated active sites. To address this issue, more attention should be paid to methods for stabilizing the nanoparticle/cluster such as stabilizing it in a porous material.

Synergy effect

After forming alloys, the catalytic performances of alloyed SACs are usually affected by various factors, thus influencing the types and binding energy of the reactants and the intermediates. The crucial structure factors affecting the catalytic performance for alloyed SACs include geometric and electronic structure. For instance, compared with pristine Ru, substitution of Ru with single Co atoms (denoted as $RuCo_1$) will reduce the energy barrier for water dissociation[32]. Meanwhile, the energy barriers will be increased when increasing the substitution to two ($RuCo_2$) or three ($RuCo_3$) neighbor Co atoms, indicating that geometrically, single Co substitution can enhance the sluggish water dissociation of both $RuCo_n$ ($n \geq 2$) and pristine Ru catalysts. Moreover, the addition of more Co atoms will increase the binding energy of OH (ΔE_{OH}), while single Co atom substitution induces a moderate ΔE_{OH}. Thus, $RuCo_1$ structure can not only facilitate water dissociation, but also prevent the deactivation of the active sites induced by high-affinity hydroxides.

Meanwhile, the charge transfer due to the differences in electronegativity as a short-range effect also alters the electronic structures and leads to the variation in binding strength of the intermediates. These effects are summarized as the electronic effects. Different from traditional alloy catalysts, no metallic bond is formed between the neighboring alloyed atoms, inducing a free-atom-like electronic structure[33], which is common for homogeneous catalysts with the ligands tuning the electron density of the metal center and thus the reactivity of the catalysts. For example, after loading Ru single atom onto $CoFe_2$(O-8)(110), charge transfer occurs from Ru to the coordinated surface $O_{lattice}$, which will induce an electron-deficient center to accelerate electrocatalytic OER and facilitate intermediate adsorption[34].

CASE STUDIES OF ALLOYED SACs FOR WATER SPLITTING

Electrocatalytic HER

Pt-based catalysts

Since Pt nanocatalysts are the most widely used electrocatalysts for HER, decorating Pt nanocatalysts with other low-cost transition metals offers an effective way to optimize their catalytic properties. Table 1 summarizes the representative applications of alloyed SACs for electrocatalytic water splitting. For instance, by starting with the PtNi nanowire and a partial electrochemical dealloying approach, single Ni atom-modified Pt nanowires demonstrated an optimum combination of electrochemical active surface area and specific activity for not only HER but also methanol oxidation and ethanol oxidation[35]. Density functional theory (DFT) calculations indicated that Ni single atoms, which are coordinated with two hydroxyl groups [Figure 4A], electronically enhanced HER activity over the neighboring Pt atoms. Single In atom-doped sub-nanometer Pt nanowires were also reported to be excellent electrocatalysts for HER under universal pH conditions[36]. Mechanistic studies indicated that the combination of single atom In decoration [Figure 4B and C] and ultrathin 1D morphology provided the maximum active sites and effectively activated Pt atoms for the reaction to occur. Pt nanoclusters as electrocatalysts for HER are normally not stable, while when

Table 1. Summary of the representative alloyed SACs for electrocatalytic HER and OER

Entry	Catalysts	Single atom	Reaction	Electrolytes	Tafel slope ($mV \cdot dec^{-1}$)	Overpotential (@10 $mA \cdot cm^{-2}$/mV)	Ref.
1	SANi-PtNWs	Ni	HER	1 M NaOH	60.3	/	[35]
2	SA In-Pt NWs	In	HER	1 M KOH	32.4	46	[36]
3	Pt/Ni ASs/C	Pt	HER	1 M KOH	47	28	[38]
4	NiPt	Pt	HER	1 M KOH	45	18	[39]
5	(Ru@Pt)–N	Pt	HER	1 M KOH	30	15	[40]
6	Pd-Pt/NCNTs	Pt	HER	/	28.5	/	[41]
7	RuAu SAA	Au	HER	1 M KOH	37	24	[42]
8	Ru SA-Co-N-C	Ru	HER	0.1 M KOH	64	43	[43]
9	$Ir_1Ni@MoO_2$	Ir	HER/OER	1 M KOH	19/91	48.6/280	[44]
10	Co-substituted Ru NSs	Co	HER	1 M KOH	29	13	[32]
11	Co/Pdm-4	Co	HER	0.5 m H_2SO_4	8.2	24.7	[46]
12	Ru_1-Pt_3Cu	Ru	OER	0.1 M $HClO_4$	/	90	[31]
13	$RuSACoFe_2/G$	Ru	OER	1 M KOH	51	80	[34]
14	$NiFeIr_x/Ni$	Ir	OER	1 M KOH	44.6	200	[57]
15	Ir@Co nanosheets	Ir	OER	1 M KOH	99	273	[58]

SACs: Single-atom catalysts; HER: hydrogen evolution reaction; OER: oxygen evolution reaction; SAA: single-atom alloy.

they were loaded onto Cr-N_4 with atomically dispersed Cr sites, both the activity and stability were enhanced, which outperforms the activity of commercial Pt/C catalysts[37]. Theoretical and experimental studies demonstrated that a unique Pt-Cr quasi-covalent bond was formed at the interface of Cr-N_4 sites, and Pt nanoclusters which effectively suppressed thermal vibration and migration of Pt atoms contributed to the significantly enhanced stability. Furthermore, exophilic Cr-N_4 sites adjacent to Pt nanoclusters demonstrated favorable adsorption for hydroxyl species, which favored water dissociation nearly barrierless and thus enhanced HER activity.

Although with high HER activity, the high price of Pt induces high costs of the catalytic systems. Atomically dispersed Pt atoms offer an opportunity to reduce the catalyst cost and promote HER activity. Ding *et al.* embedded isolated Pt atoms into hexagonal close-packed and anisotropic super-structured nickel (Pt/Ni, Figure 4D-F) to enhance HER performance in 1 M KOH, with the overpotential of 28.0 mV at 10 $mA \cdot cm^{-2}$ over Pt/Ni catalyst which is superior to that of 71.0 mV over Pt/C[38]. The Tafel slope of 47.0 $mV \cdot dec^{-1}$ shows the Volmer-Heyrovsky mechanism over the Pt/Ni catalyst. DFT calculations show that the adsorption free energy over the Pt-Ni-hcp model is much higher than on Ni-hcp [Figure 4G], indicating that hydrogen adsorption is favorable over Ni sites, while H_2 desorption is favored over Pt sites. Thus, the improved HER activity over Pt/Ni can be explained by a dissociation-diffusion-desorption mechanism [Figure 4H]: due to the dissociation of H_2O, H was firstly adsorbed over Ni, and then diffused to Pt sites, followed by H_2 release from Pt sites. The synergy effects between Ni-Pt and Ni-Ni, which are responsible for excellent HER activity, are working for Pt single-atom-promoted Ni nanosheets as well, with the activity significantly outperforming that of commercial Pt/C[39]. Likewise, Ru doped with Pt single atoms also demonstrated promoted desorption of H_2. N-doped Pt-Ru alloy with isolated Pt atoms was synthesized via thermal annealing under ammonium atmosphere[40]; after optimization of the studied catalysts, (Ru-N)@Pt with Ru-N-Pt structure displayed the best HER activity. The high activity can be ascribed to the incorporated N, which can regulate Ru orbital, thus accelerating water dissociation, and Pt single atoms favored H_2 desorption.

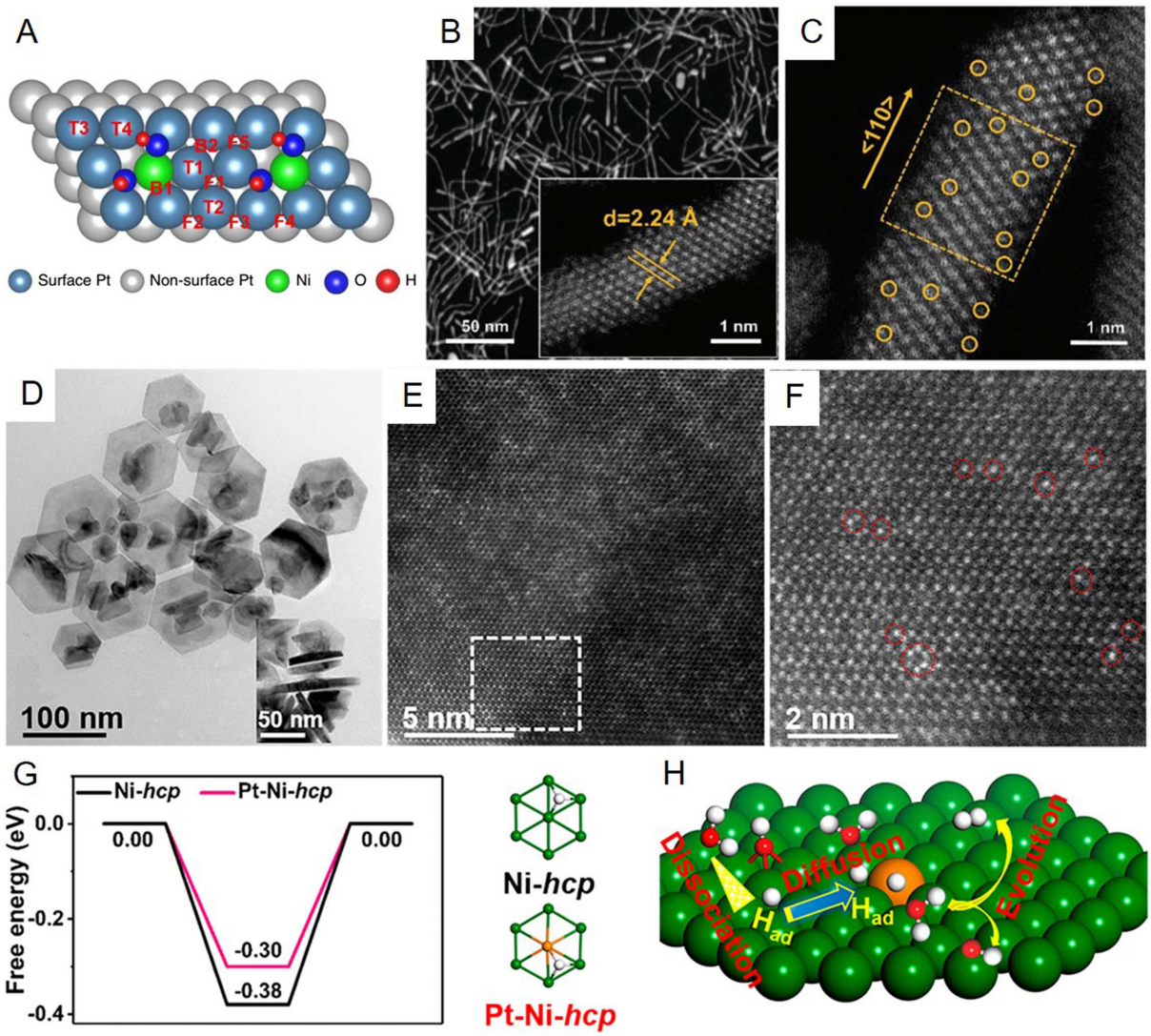

Figure 4. (A) Model for single-atom Ni-decorated Pt (111) surface, with the Ni atoms in the surface layer. This figure is quoted with permission from ref[35]. Copyright 2019, Springer Nature; (B) HAADF-STEM image and (C) aberration-corrected HAADF-STEM image for single atom In decorated Pt nanowires. Figures are quoted with permission from ref[36]. Copyright 2020, Wiley-VCH; (D) TEM image of the Pt/Ni catalyst, (E) HAADF-STEM image and (F) magnified aberration-corrected image obtained from the white square in (E); (G) free adsorption energies of H over Pt-Ni-hcp and Ni-hcp; (H) corresponding dissociation–diffusion–desorption mechanism for hydrogen evolution over Pt-Ni-hcp. Figures are quoted with permission from ref[38]. Copyright 2021, American Chemical Society. HAADF-STEM: High-angle annular dark field scanning transmission electron microscopy; TEM: transmission electron microscopy.

Pt/Pd alloy with isolated Pt over Pd octahedrons, which was prepared by an atomic layer deposition method, was employed to enhance the electrocatalytic HER performance[41]. X-ray absorption near-edge structure (XANES) study showed that different from other catalysts, the density of 5d states was highly unoccupied for Pt atoms. Pt/Pd alloy with octahedral structure and single Pt atoms displayed significantly enhanced ORR and HER activity compared with those of the cubic Pt/Pd alloy, Pd octahedral and pristine Pt. The Tafel slope of 28.5 mV·dec^{-1} indicates the Volmer-Tafel mechanism for water splitting. DFT study demonstrated that H^+ was strongly adsorbed by Pt atoms over Pd(111), and the adsorption of followed two H species would be promoted due to the Pt atoms with the highly unoccupied density of 5d states. Since the increased H coverage would decrease H adsorption energy, it favors the H_2 molecule formation. The calculated data also demonstrated a narrower Pt single atom projected density of d state in Pt/Pd than that

of Pt(111), indicating the electronic structure changes due to the synergy effects in the alloy.

Non-Pt-based HER catalysts

Non-Pt-based catalysts gained great attention for electrocatalytic HER. Their single-atom decoration to form alloys also holds significant potential for HER. Chen *et al.* managed to disperse isolated Au atoms onto Ru via a laser ablation technique in a liquid phase[42]. RuAu alloy showed much lower overpotential than that of Pt (24 *vs.* 46 mV at 10 $mA \cdot cm^{-2}$ in 1 M KOH, respectively). The Tafel slope of 37 $mV \cdot dec^{-1}$ indicates the Volmer-Heyrosky mechanism for HER over RuAu alloy. DFT study was performed to investigate the adsorbed species evolution during the reaction, which demonstrated that RuAu alloy displayed moderate water dissociation and H_2 desorption capability, while poor water dissociation capability was found over Pt and strong hydrogen binding was verified over Ru. Owing to the electronic structure changes after the formation of AuRu alloy, H adsorption and H_2 molecule formation were promoted over negative Au sites, while H_2O adsorption was favored over positive Ru atoms; Au and Ru played synergetic roles in different orders during the reaction which resulted from the optimized electronic effects. Meanwhile, Ru can also act as an active promoter for HER; by constructing Ru single atom-decorated Co nanoparticles into carbon sheath, a Ru SA-Co-N-C catalyst was fabricated [Figure 5A-C] which demonstrated an exceptionally high catalytic performance for overall water splitting, with an outstanding mass activity of 1,251 $mA \cdot mg_{Ru}^{-1}$ and a minimal cell voltage of 1.55 V at 10 $mA \cdot cm^{-2}$[43]. DFT calculations [Figure 5D and E] further verified that the Ru SA-Co-N-C catalyst could effectively optimize the adsorption energy of the intermediates, such as H^*, OH^*, O^*, and OOH^*, making almost thermoneutral electrocatalysis with the composite materials.

Ir-based catalysts were also recognized as efficient catalysts for water splitting. The most recent work from Wang *et al.* demonstrated that single-atom Ir-decorated nickel supported on segregated MoO_2 showed a low overpotential of 48.6 mV at 10 $mA \cdot cm^{-2}$, with a Tafel slope of 19 $mV \cdot dec^{-1}$ for HER[44]. Experimental and theoretical studies revealed that the Ir-Ni interface significantly weakens the binding energy of H, and Ir single-atom decoration boosted the surface reconstruction of Ni species, and thus enhanced the intermediates (OH^*) coverage and optimized the potential-determining step. However, the study on Ir-based alloyed SACs for water splitting is very limited; owing to the high activity of Ir-based electrocatalysts, more attention is needed for alloying single atom Ir with other elements to boost water splitting activity, which will help the design of highly efficient water splitting catalysts.

To help the design of efficient HER catalysts, Zhou *et al.* conducted theoretical prediction of a series of binary/ternary metallic catalysts[45]. Considering the cost and stability and the location of single atoms, Ni-based catalysts with atomically dispersed Ni were predicted to be efficient for HER, as verified by the subsequent experimental study on the HER activity over the synthesized Ni-based alloyed SACs. Meanwhile, more experimental studies are needed to screen high-performance HER catalysts. Besides, a highly stable and active Co-substituted Ru nanosheet was synthesized[32] that demonstrated an extremely low overpotential of 13 mV at 10 $mA \cdot cm^{-2}$ in 1 M KOH. The ultralow Tafel slope of 29 $mV \cdot dec^{-1}$ outperformed those of other reported Pt-free electrocatalysts. DFT study revealed that the water dissociation energy barrier was greatly reduced after single Co atom substitution, which is the main reason for its superior HER performance. Another example is Co single atoms immobilized on Pd-based nanosheets[46], where the unsaturated coordination environments and unique electronic and geometric structures modulated the redistribution of charges and the *d*-band center, leading to highly active electronic states on the catalyst surface. The catalyst displayed outstanding HER activity in both alkaline and acid conditions, with a low overpotential of 24.7 mV at 10 $mA \cdot cm^{-2}$ and a Tafel slope of 8.2 $mV \cdot dec^{-1}$ in the acidic medium, which are superior to those of commercial Pd/C and Pt/C.

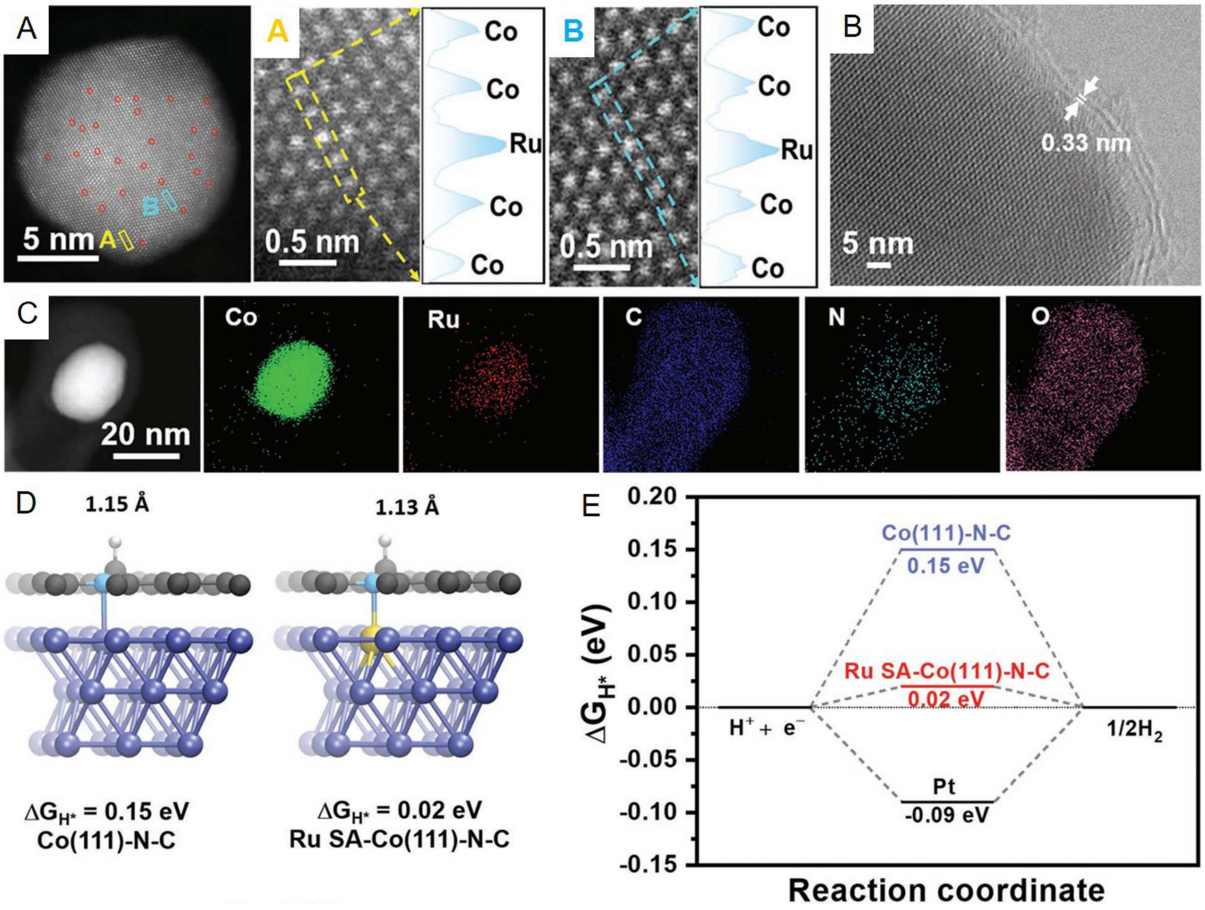

Figure 5. (A) HAADF-STEM image of Ru SA-Co-N-C, and the corresponding element contrast in randomly selected region (yellow A and blue B); (B) HRTEM image, (C) HAADF-STEM image, and the corresponding STEM-EDS of Ru SA-Co-N-C; (D) side views of atomic H adsorption on the Co-N-C and Ru SA-Co-N-C surfaces; (E) calculated free energy diagram on Co-N-C, Ru SA-Co-N-C and Pt for hydrogen evolution. Figures are quoted with permission from ref[43]. Copyright 2022, Wiley-VCH. HAADF-STEM: High-angle annular dark field scanning transmission electron microscopy; HRTEM: high-resolution transmission electron microscopy; STEM-EDS: scanning transmission electron microscopy-energy dispersive X-ray spectroscopy.

Nanoclusters prepared with atomic precision

Recently, catalytic application of metallic nanoclusters with atomic precision makes it possible for precise investigation of the structure-activity relationship[47]. Through single-atom doping/substitution, influence of single atoms in an alloy has been precisely studied for electrocatalytic HER[48,49]. Pt single atom substitution is the most widely investigated modification in nanoclusters for electrocatalytic HER[50-54]. For instance, Kwak *et al.* synthesized a bimetallic nanocluster of $PtAu_{24}(SC_6H_{13})_{18}$ by single Pt atom substitution of $Au_{25}(SC_6H_{13})_{18}$; the bimetallic nanocluster showed excellent activity for H_2 production, superior to any other molecular catalysts and the benchmarking Pt catalyst[50]. Mechanism study [Figure 6A] indicated that H binding step over the bimetallic nanocluster is thermodynamically neutral, Pt-H chemical bonds can be formed with the central doped Pt atom. Besides Pt single atom doping, substitutions of other single atom metal elements (Pd, Ag, Cu, *etc.*) were also reported to demonstrate enhanced HER activity[53-55]. The interactions of hydrogen with $[Au_{25}(SR)_{18}]^q$ and single atom-doped bimetallic $[MAu_{24}(SR)_{18}]^q$ (M = Pt, Pd, Cu, Ag, Cd, or Hg) nanoclusters were investigated by theoretical study[53], which demonstrated that hydrogen behaves as a metal in the nanoclusters and its 1*s* electron contributes to their super atomic free-electron count; combined with the calculated hydrogen adsorption free energy (ΔG_H), center-doped $CuAu_{24}(SR)_{18}$, $Pd_1Au_{24}(SR)_{18}$ and $Pt_1Au_{24}(SR)_{18}$ were predicted to be good catalysts for HER. The

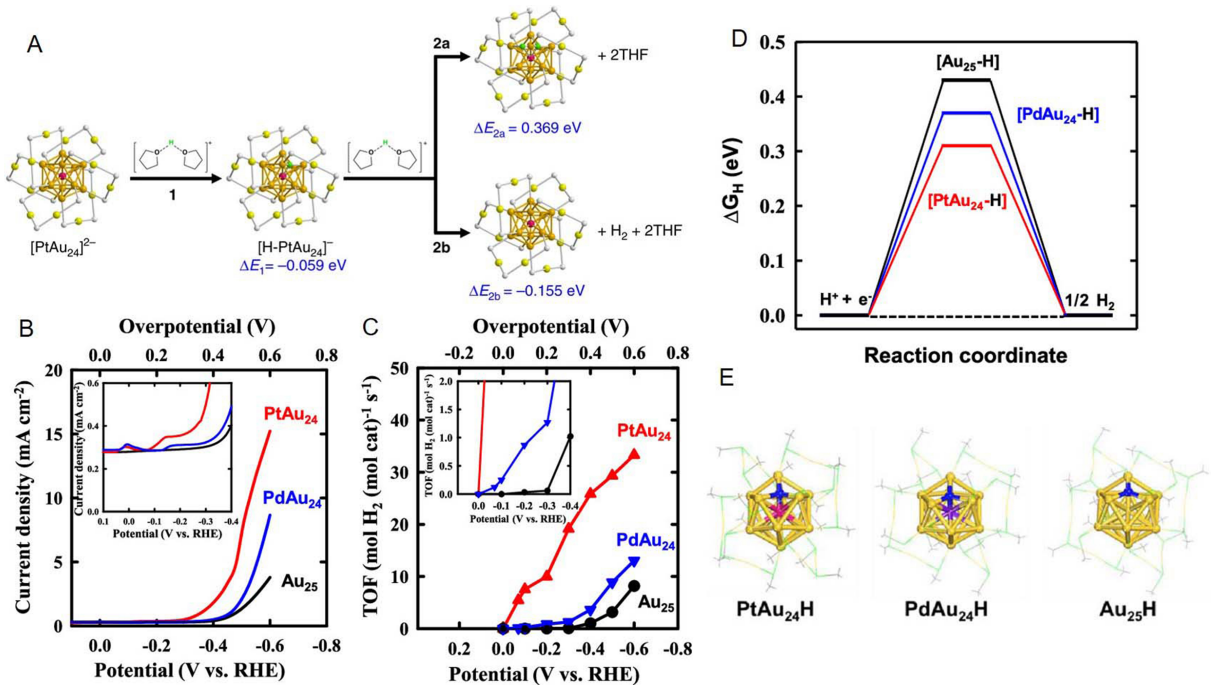

Figure 6. (A) Calculated reaction energies for HER over Pt_1Au_{24} nanocluster. Figures are quoted with permission from ref[50]. Copyright 2017, Springer Nature; (B) Linear sweep voltammetry and (C) plots of turnover frequency vs. potential over different nanoclusters; (D) calculated ΔG_H diagram for hydrogen adsorption with the order consistent to their HER activities; and (E) the optimized structure for different nanoclusters interacted with hydrogen. Figures are quoted with permission from ref[54], Copyright 2018, American Chemical Society. HER: Hydrogen evolution reaction.

experimental study [Figure 6B and C] indeed demonstrated an order of Pt_1Au_{24} > Pd_1Au_{24} > Au_{25} for both the catalytic turnover frequency (TOF) and current density of electrocatalytic HER[54], which is consistent with the calculated ΔG_H [Figure 6D and E].

Electrocatalytic OER

For electrocatalytic water splitting, oxygen evolution proceeds via a sluggish four-electron transfer process. Among the studied catalysts, Ru is compared to other noble metals relatively abundant, and RuO_2 displays superior catalytic activity for OER compared with other noble metal oxide catalysts. However, the stability of RuO_2 catalysts was not satisfied due to the dissolution of Ru via soluble ruthenate species. To enhance the stability of Ru-based catalysts for OER, Yao *et al.* synthesized isolated Ru atoms over a Pt-Cu host [Figure 7A-D][31]. Strains were generated by controlling the compositions of Pt-Cu hosts, and then contributed to OER catalytic performance of Ru single atoms. Owing to the moderate adsorbate binding energy over Ru single atoms, Ru_1-Pt_3Cu demonstrated the best OER catalytic performance [Figure 7E] among the studied catalysts. Meanwhile, the stability of the Ru_1-Pt_3Cu catalyst was also significantly enhanced [Figure 7F], which could be attributed to the formation of compressive strain, thus suppressing the overoxidation of Ru atoms. Compared with other catalysts, the superior OER activity over Ru_1-Pt_3Cu can be ascribed to the modest free energies of the intermediates of OH^* and O^* [Figure 7G]. This study demonstrated that the electronic structure of alloyed single atoms can further be optimized by using bimetallic hosts to change the catalytic activity.

Non-noble transition metals are normally used for OER especially under alkaline conditions[56], which can remarkably reduce the catalyst cost. After further modification by noble metal with atomic dispersion, the coordination environments were optimized for enhancing the OER catalytic performance. Lee *et al.*

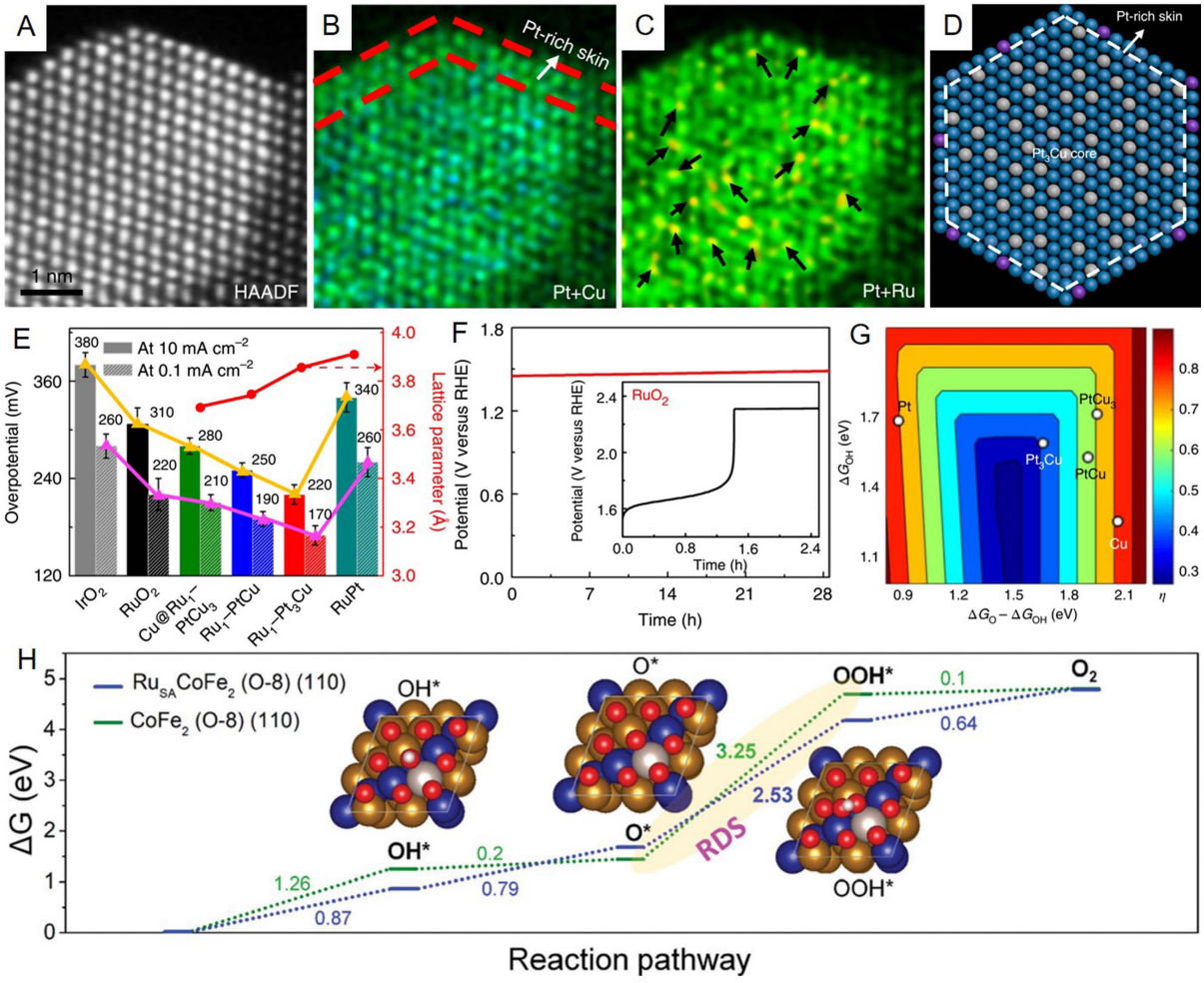

Figure 7. (A-C) Elemental mapping of Ru_1-Pt_3Cu with atomic resolution; (D) the corresponding schematic atom model; (E) overpotential for the catalysts to reach 0.1 and 10 mA·cm^{-2}; (F) chronopotentiometric tests for Ru_1-Pt_3Cu and RuO_2 at 10 mA·cm^{-2}; (G) calculated volcano plot for the OER overpotential. Figures are quoted with permission from ref[31], Copyright 2019, Springer Nature; (H) The calculated profiles for the free energy during OER over different catalyst surfaces. Figures are quoted with permission from ref[34], Copyright 2020, Royal Society of Chemistry. OER: Oxygen evolution reaction.

managed to disperse Ru single atoms over the $CoFe_2$ surface to get the catalyst named $RuSACoFe_2$/G, which demonstrated a much lower overpotential of 180 mV at 10 mA·cm^{-2} than those of RuO_2 and $CoFe_2$ (298 and 313 mV, respectively)[34]. The enhanced catalytic performance of $RuSACoFe_2$/G has been ascribed to the reduced energy barrier for the rate-limiting step, with the isolated Ru atoms stabilizing the OOH* intermediate and oxygen species pre-adsorbed on Co-Fe [Figure 7H].

Other than Ru-based catalysts, isolated Ir atoms were also verified to display excellent OER activity[57,58]. With isolated Ir atoms anchored onto 3D amorphous NiFe nanowire@nanosheets to form the $NiFeIr_x$/Ni catalysts, over 12 h long-term stability and decreased overpotential of 200 mV at 10 mA·cm^{-2} were obtained[57]. The significantly enhanced OER performance has been attributed to the synergy effect between isolated Ir atoms on NiFe/Ni support. Owing to the stabilization of OOH* species and the synergy effect between Ir-Co dual-sites, Ir single atoms-decorated Co nanoparticles have been reported to show superior OER activity than monometallic Ir catalysts[58]. These studies demonstrated that the formation of alloyed single atoms can display superior electrocatalytic OER activity.

Up to now, the study on alloyed SACs for OER is very limited; continued efforts are urgently needed for high-performance OER catalysts with isolated and alloyed metal sites. To improve the activity and stability of the catalysts, special support can be chosen; for example, a recent study showed that metal-organic frameworks (MOFs) were promising for stabilizing bimetallic atoms with atomic precision for OER[59].

Photocatalytic HER

Solar-driven water splitting to produce hydrogen and oxygen is among the possible avenues for sustainable and carbon-free energy generation[29], which can simultaneously alleviate the current environmental and energy issues. The formation of alloyed Pt single atoms with other metal elements has been reported to demonstrate high efficiency for solar-driven HER[60-62]. By using a one-unit-cell of $ZnIn_2S_4$ (ZIS) nanosheet with abundant Cu as dopants, a single atom Pt alloyed Cu catalyst (Pt_1/Cu-ZIS) was obtained [Figure 8A-C], which showed a notable solar-driven HER rate of 5.02 $mmol \cdot g^{-1} \cdot h^{-1}$; the value is nearly 5, 15, and 48 times higher than those of Pt_{nc}/ZIS, Cu-ZIS, and pristine ZIS, respectively[60]. Control experiments, combined with various advanced characterizations and DFT calculations, confirmed that Cu dopants can not only stabilize the isolated Pt atoms, but also promote the photogenerated electron transfer efficiency. Meanwhile, Cu dopants acted as surface trap centers to capture photogenerated electrons from the conduction band after photoexcitation [Figure 8D-G]. Thus, the formation of alloyed Pt single atoms with Cu serves as the electron transfer channel to enhance the electron transfer for driving water splitting. Another example comes from a bimetallic nanoparticles/MOF system[61], where Pt single atoms are alloyed with Pd to form Pd@Pt/UiO-66-NH_2. The Pt shell on Pd can be precisely controlled, with the structure varying from core-shell to single atom distribution, thus changing the coordination environment of Pt. Consequently, the surface charge of Pd and Pt can be redistributed [Figure 8H], which optimized the electronic state of the active sites to enhance photocatalytic HER activity.

Besides the conventional Pt-based co-catalysts, bimetallic nanoclusters with atomic precision have received increasing attention[47]. For instance, the work from Du *et al.* demonstrated enhanced photocatalytic HER activity over $Pt_1Ag_{24}(SR)_{18}$/g-C_3N_4 [Figure 9A]; the hydrogen evolution rate was significantly higher than those of pristine g-C_3N_4 and $Ag_{24}(SR)_{18}$/g-C_3N_4 (330 and four times, respectively)[62] [Figure 9B]. The semicircle in the Nyquist plot for Pt_1Ag_{24}/g-C_3N_4 was significantly reduced [Figure 3A], suggesting a small transfer barrier of photogenerated charges, indicating that Pt single atom doping can seriously optimizing the photogenerated charge carrier dynamics, thus enhancing the photocatalytic HER activity of $Ag_{24}(SR)_{18}$/g-C_3N_4. With $Ag_{19}Pt_1$ as a model, investigation on quantum dynamics for the photogenerated charges and structural dynamics for plasmon-assisted solar-driven water splitting was undertaken at the atomic length scale and femtosecond time scale[63], which demonstrated that the interaction of water with the nanocluster would be enhanced mainly due to Pt single atom substitution on tip atoms of the tetrahedral Ag_{20} nanocluster. The photogenerated electron transfer would also be enhanced, thus accelerating the charge transfer to enhance water splitting activity.

Charge transfer can be promoted by optimizing the interface between the semiconductor and co-catalyst, which will reduce the recombination of photogenerated electron-hole pairs. By loading $Pt_1Ag_{24}(SR)_{18}$ or $Pd_1Au_{24}(SR)_{18}$ onto $BaLa_4Ti_4O_{15}$, the effect of single Pt or Pd atom doping affecting photoelectrochemical water splitting activity was investigated[64], which demonstrated that single Pt atom doping would enhance the photocatalytic water splitting activity, while doping with Pd lowered the activity. Structure analysis showed that Pd atoms were located at the nanocluster surface, while Pt atoms were loaded at the interface of $BaLa_4Ti_4O_{15}$ and the nanoclusters [Figure 9C], which considerably affects the photoelectrochemical activity [Figure 9D].

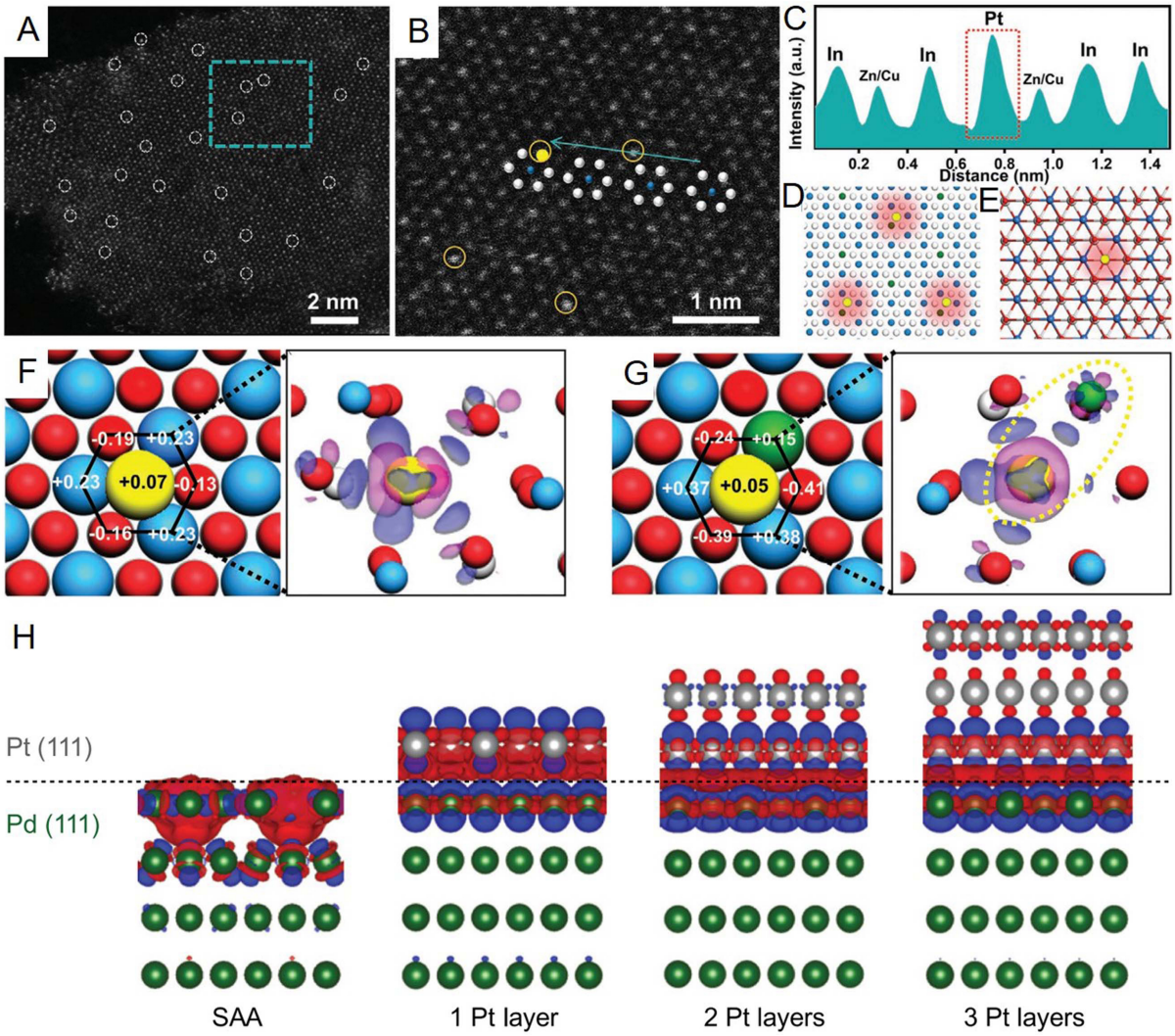

Figure 8. (A) Atomic-resolution HAADF-STEM image of Pt_1/Cu-ZIS with white circle showing the Pt single atoms; (B) representative HAADF-STEM image with (C) the intensity profile of the dark cyan arrow in (B); (D and E) the crystal structure of Pt_1/Cu-ZIS, Mulliken charge analysis and the density difference of Pt atoms adsorbed over (F) ZIS and (G) Cu-ZIS. Figures are quoted with permission from ref[60], Copyright 2021, Wiley-VCH; (H) Calculated differential charge density indicated the charge redistribution of the Pd@Pt nanoparticles with SAA structure and core-shell structure of different Pt layers. Figures are quoted with permission from ref[61], Copyright 2021, Natl. Sci. Rev. HAADF-STEM: High-angle annular dark field scanning transmission electron microscopy; ZIS: $ZnIn_2S_4$; SAA: single-atom alloy.

However, results might be confusing for the Ag_{25} nanoclusters; when doped with Pt, Pd and Au and then loaded onto TiO_2, the catalytic activity follows an order of $Ag_{25} \geq PtAg_{24} > PdAg_{24} \geq AuAg_{24}$ [65]. With the geometric structure well-preserved after doping, the electronic structures of the nanoclusters were significantly altered. DFT calculations and ultraviolet photoelectron spectroscopy (UPS) measurements led to the conclusion that the mismatched energy levels between TiO_2 and the doped nanoclusters were responsible for the lower activities. While, further detailed study is still needed for the underpinning reasons for the activity difference.

Besides the above-mentioned studies, less attention has been paid to photocatalytic OER. Compared to light-driven HER, photocatalytic OER would be more difficult. Transition metal oxide co-catalysts are normally efficient for photocatalytic OER. Thus, future study of alloyed single atom structures loaded onto

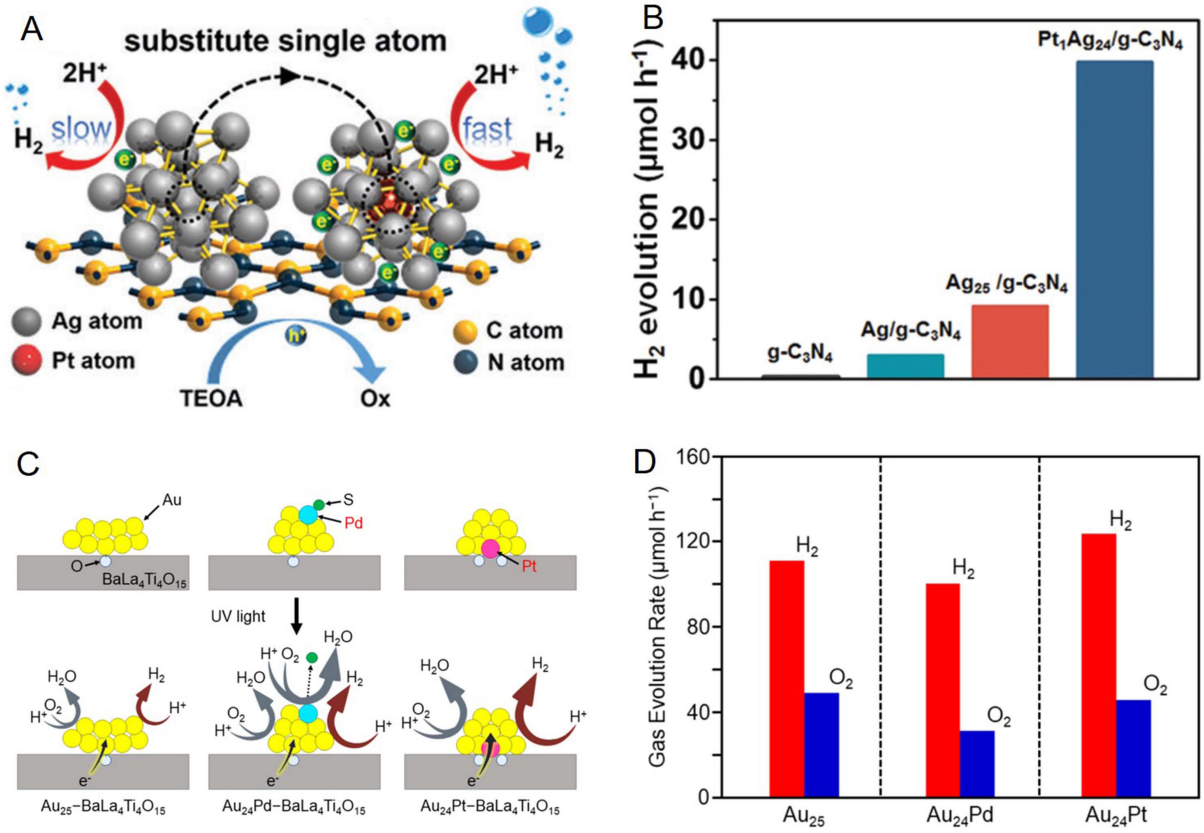

Figure 9. (A) The possible photocatalytic H_2 evolution mechanism; (B) photocatalytic HER performance of different catalysts. Figures are quoted with permission from ref[62], Copyright 2017, the Royal Society of Chemistry; (C) Proposed structures of the catalysts before (top) and during (bottom) water splitting process; (D) Photocatalytic water splitting for the generation of H_2 and O_2 over different catalysts. Figures are quoted with permission from ref[64], Copyright 2019, American Chemical Society. HER: Hydrogen evolution reaction.

such metal oxides might enhance the photocatalytic OER performance.

CONCLUSION AND OUTLOOK

Catalysts that alloy single metal atoms with another host metal offer the dual merits of maximizing the metal atom utilization of SACs and the synergy effect of metallic alloy catalysts. This combination can lead to significantly enhanced catalytic activity and improved long-term stability for water splitting to produce hydrogen and oxygen. The principle of alloyed SACs for their enhanced catalytic performance for electrocatalytic HER/OER and photocatalytic HER was especially discussed and compared to gain insight into the catalytic mechanism. However, despite many studies conducted on these catalysts for water splitting, multiple factors still need to be addressed to make them viable for practical application.

1. To control and maintain the uniform atomic distribution of single atoms in alloyed SAC is still challenging, though many synthetic strategies have been developed. Novel methods for simple and large-scale production of alloyed SACs are still needed urgently. Additionally, special attention needs to be paid to the deposition of the catalysts to make them more active for electrocatalysis.

2. Obviously, most studies for water splitting over alloyed SACs focus on HER; limited attention has been paid to OER, especially under photocatalytic conditions. Much more attention should be paid to developing

alloyed SACs for electro/photocatalytic OER.

3. Current studies on the kinds of alloyed SACs are still very limited. Rational design and extension of other metal elements (i.e., Ir, Fe) and multi-metal alloys (i.e., high-entropy alloy)-based catalysts hold great potential for highly efficient water splitting reaction.

4. Besides the structure characterization, *in situ*/*operando* study of the structure changing of the catalysts and the gaseous products evolution of water splitting reaction are important for optimizing the activity/stability of specific catalysts and understanding the catalytic mechanism.

5. In addition to traditional theoretical prediction, machine learning and artificial intelligence (AI) are recently emerging computer-related approaches that are promising for providing theoretical guidance for rational design and catalytic mechanism clarification of alloyed SACs; special attention is needed for these aspects.

Although many challenges remained, increased enthusiasm for investigating alloyed SACs for water splitting holds promise for the development of novel catalysts to enhance the catalytic performance, which is expected to lead to substantial improvements and innovations in catalytic technologies for sustainable energy solutions.

DECLARATIONS

Authors' contributions

Investigated all the literature and designed and wrote the manuscript: Pei, G. X.
Contributed to the critical discussion for revising the manuscript: Qi, H.; Hofmann, J. P.
The final version of the manuscript has been approved by all authors.

Availability of data and materials

Not applicable.

Financial support and sponsorship

This work was supported by the Natural Science Foundation of Shandong Province (No. ZR2023QB178). Qi, H. thanks the Marie Skłodowska-Curie Actions Postdoctoral Fellowships (101107009-AtomCat4Fuel) and UKRI (EP/Y029305/1).

Conflicts of interest

All authors declared that there are no conflicts of interest.

Ethical approval and consent to participate

Not applicable.

Consent for publication

Not applicable.

REFERENCES

1. Miao, L.; Jia, W.; Cao, X.; Jiao, L. Computational chemistry for water-splitting electrocatalysis. *Chem. Soc. Rev.* **2024**, *53*, 2771-807. DOI PubMed
2. Wei, S.; Sacchi, R.; Tukker, A.; Suh, S.; Steubing, B. Future environmental impacts of global hydrogen production. *Energy. Environ. Sci.* **2024**, *17*, 2157-72. DOI
3. Zhao, L.; Wang, S.; Liang, S.; An, Q.; Fu, J.; Hu, J. Coordination anchoring synthesis of high-density single-metal-atom sites for electrocatalysis. *Coord. Chem. Rev.* **2022**, *466*, 214603. DOI
4. Nakaya, Y.; Furukawa, S. Catalysis of alloys: classification, principles, and design for a variety of materials and reactions. *Chem. Rev.* **2023**, *123*, 5859-947. DOI PubMed
5. Liu, L.; Corma, A. Bimetallic sites for catalysis: from binuclear metal sites to bimetallic nanoclusters and nanoparticles. *Chem. Rev.* **2023**, *123*, 4855-933. DOI PubMed PMC
6. Yun, Q.; Lu, Q.; Li, C.; et al. Synthesis of PdM (M = Zn, Cd, ZnCd) nanosheets with an unconventional face-centered tetragonal phase as highly efficient electrocatalysts for ethanol oxidation. *ACS. Nano.* **2019**, *13*, 14329-36. DOI
7. Zhang, Z.; Liu, G.; Cui, X.; et al. Crystal phase and architecture engineering of lotus-thalamus-shaped Pt-Ni anisotropic superstructures for highly efficient electrochemical hydrogen evolution. *Adv. Mater.* **2018**, *30*, 1801741. DOI
8. Zhu, J.; Elnabawy, A. O.; Lyu, Z.; et al. Facet-controlled Pt–Ir nanocrystals with substantially enhanced activity and durability towards oxygen reduction. *Mater. Today.* **2020**, *35*, 69-77. DOI
9. Kyriakou, G.; Boucher, M. B.; Jewell, A. D.; et al. Isolated metal atom geometries as a strategy for selective heterogeneous hydrogenations. *Science* **2012**, *335*, 1209-12. DOI
10. Hannagan, R. T.; Giannakakis, G.; Flytzani-Stephanopoulos, M.; Sykes, E. C. H. Single-atom alloy catalysis. *Chem. Rev.* **2020**, *120*, 12044-88. DOI PubMed
11. Mao, J.; Yin, J.; Pei, J.; Wang, D.; Li, Y. Single atom alloy: an emerging atomic site material for catalytic applications. *Nano. Today.* **2020**, *34*, 100917. DOI
12. Zhang, T.; Walsh, A. G.; Yu, J.; Zhang, P. Single-atom alloy catalysts: structural analysis, electronic properties and catalytic activities. *Chem. Soc. Rev.* **2021**, *50*, 569-88. DOI
13. Sun, X.; Song, Y.; Jiang, G.; Lan, X.; Xu, C. Fundamentals and catalytic applications of single-atom alloys. *Sci. China. Mater.* **2024**, *67*, 1-17. DOI
14. Pei, G.; Liu, X.; Chai, M.; Wang, A.; Zhang, T. Isolation of Pd atoms by Cu for semi-hydrogenation of acetylene: effects of Cu loading. *Chin. J. Catal.* **2017**, *38*, 1540-8. DOI
15. Pei, G. X.; Liu, X. Y.; Yang, X.; et al. Performance of Cu-alloyed Pd single-atom catalyst for semihydrogenation of acetylene under simulated front-end conditions. *ACS. Catal.* **2017**, *7*, 1491-500. DOI
16. Pei, G. X.; Liu, X. Y.; Wang, A.; et al. Ag alloyed Pd single-atom catalysts for efficient selective hydrogenation of acetylene to ethylene in excess ethylene. *ACS. Catal.* **2015**, *5*, 3717-25. DOI
17. Pei, G. X.; Liu, X. Y.; Wang, A.; et al. Promotional effect of Pd single atoms on Au nanoparticles supported on silica for the selective hydrogenation of acetylene in excess ethylene. *New. J. Chem.* **2014**, *38*, 2043. DOI
18. Shen, T.; Wang, S.; Zhao, T.; Hu, Y.; Wang, D. Recent advances of single-atom-alloy for energy electrocatalysis. *Adv. Energy. Mater.* **2022**, *12*, 2201823. DOI
19. Da, Y.; Jiang, R.; Tian, Z.; Han, X.; Chen, W.; Hu, W. The applications of single-atom alloys in electrocatalysis: progress and challenges. *SmartMat* **2023**, *4*, e1136. DOI
20. Zhuang, J.; Wang, D. Recent advances of single-atom alloy catalyst: properties, synthetic methods and electrocatalytic applications. *Mater. Today. Catal.* **2023**, *2*, 100009. DOI
21. Gao, Q.; Han, X.; Liu, Y.; Zhu, H. Electrifying energy and chemical transformations with single-atom alloy nanoparticle catalysts. *ACS. Catal.* **2024**, *14*, 6045-61. DOI PubMed PMC
22. Ahmed, M.; Wang, C.; Zhao, Y.; et al. Bridging together theoretical and experimental perspectives in single-atom alloys for electrochemical ammonia production. *Small* **2024**, *20*, 2308084. DOI
23. Gao, Q.; Yao, B.; Pillai, H. S.; et al. Synthesis of core/shell nanocrystals with ordered intermetallic single-atom alloy layers for nitrate electroreduction to ammonia. *Nat. Synth.* **2023**, *2*, 624-34. DOI
24. Cao, Y.; Chen, S.; Bo, S.; et al. Single atom Bi decorated copper alloy enables C-C coupling for electrocatalytic reduction of CO_2 into C_{2+} products. *Angew. Chem. Int. Ed. Engl.* **2023**, *62*, 202303048. DOI
25. Wang, J.; Xin, S.; Xiao, Y.; et al. Manipulating the water dissociation electrocatalytic sites of bimetallic nickel-based alloys for highly efficient alkaline hydrogen evolution. *Angew. Chem. Int. Ed. Engl.* **2022**, *61*, 202202518. DOI
26. Wang, H.; Zhang, K. H. L.; Hofmann, J. P.; de la Peña O'shea, V. A.; Oropeza, F. E. The electronic structure of transition metal oxides for oxygen evolution reaction. *J. Mater. Chem. A.* **2021**, *9*, 19465-88. DOI
27. Hansen, J. N.; Prats, H.; Toudahl, K. K.; et al. Is there anything better than Pt for HER? *ACS. Energy. Lett.* **2021**, *6*, 1175-80. DOI PubMed PMC
28. Zhu, J.; Hu, L.; Zhao, P.; Lee, L. Y. S.; Wong, K. Y. Recent advances in electrocatalytic hydrogen evolution using nanoparticles. *Chem. Rev.* **2020**, *120*, 851-918. DOI
29. Zhang, Z.; Yates, J. T. Jr. Band bending in semiconductors: chemical and physical consequences at surfaces and interfaces. *Chem. Rev.* **2012**, *112*, 5520-51. DOI PubMed

30. Ding, C.; Shi, J.; Wang, Z.; Li, C. Photoelectrocatalytic water splitting: significance of cocatalysts, electrolyte, and interfaces. *ACS. Catal.* **2017**, *7*, 675-88. DOI
31. Yao, Y.; Hu, S.; Chen, W.; et al. Engineering the electronic structure of single atom Ru sites via compressive strain boosts acidic water oxidation electrocatalysis. *Nat. Catal.* **2019**, *2*, 304-13. DOI
32. Mao, J.; He, C. T.; Pei, J.; et al. Accelerating water dissociation kinetics by isolating cobalt atoms into ruthenium lattice. *Nat. Commun.* **2018**, *9*, 4958. DOI PubMed PMC
33. Greiner, M. T.; Jones, T. E.; Beeg, S.; et al. Free-atom-like d states in single-atom alloy catalysts. *Nat. Chem.* **2018**, *10*, 1008-15. DOI
34. Lee, J.; Kumar, A.; Yang, T.; et al. Stabilizing the OOH^* intermediate *via* pre-adsorbed surface oxygen of a single Ru atom-bimetallic alloy for ultralow overpotential oxygen generation. *Energy. Environ. Sci.* **2020**, *13*, 5152-64. DOI
35. Li, M.; Duanmu, K.; Wan, C.; et al. Single-atom tailoring of platinum nanocatalysts for high-performance multifunctional electrocatalysis. *Nat. Catal.* **2019**, *2*, 495-503. DOI
36. Zhu, Y.; Zhu, X.; Bu, L.; et al. Single-atom in-doped subnanometer Pt nanowires for simultaneous hydrogen generation and biomass upgrading. *Adv. Funct. Mater.* **2020**, *30*, 2004310. DOI
37. Zeng, L.; Zhao, Z.; Huang, Q.; et al. Single-atom Cr-N_4 sites with high oxophilicity interfaced with Pt atomic clusters for practical alkaline hydrogen evolution catalysis. *J. Am. Chem. Soc.* **2023**, *145*, 21432-41. DOI
38. Ding, J.; Ji, Y.; Li, Y.; Hong, G. Monoatomic platinum-embedded hexagonal close-packed nickel anisotropic superstructures as highly efficient hydrogen evolution catalyst. *Nano. Lett.* **2021**, *21*, 9381-7. DOI
39. Huo, L.; Jin, C.; Tang, J.; et al. Ultrathin NiPt single-atom alloy for synergistically accelerating alkaline hydrogen evolution. *ACS. Appl. Energy. Mater.* **2022**, *5*, 15136-45. DOI
40. Luo, M.; Cai, J.; Zou, J.; Jiang, Z.; Wang, G.; Kang, X. Promoted alkaline hydrogen evolution by an N-doped Pt–Ru single atom alloy. *J. Mater. Chem. A.* **2021**, *9*, 14941-7. DOI
41. Zhang, L.; Liu, H.; Liu, S.; et al. Pt/Pd single-atom alloys as highly active electrochemical catalysts and the origin of enhanced activity. *ACS. Catal.* **2019**, *9*, 9350-8. DOI
42. Chen, C.; Wu, D.; Li, Z.; et al. Ruthenium-based single-atom alloy with high electrocatalytic activity for hydrogen evolution. *Adv. Energy. Mater.* **2019**, *9*, 1803913. DOI
43. Tong, Y.; Liu, J.; Wang, L.; et al. Carbon-shielded single-atom alloy material family for multi-functional electrocatalysis. *Adv. Funct. Mater.* **2022**, *32*, 2205654. DOI
44. Wang, B.; Li, J.; Li, D.; et al. Single atom iridium decorated nickel alloys supported on segregated MoO_2 for alkaline water electrolysis. *Adv. Mater.* **2024**, *36*, e2305437. DOI
45. Zhou, C.; Zhao, J. Y.; Liu, P. F.; et al. Towards the object-oriented design of active hydrogen evolution catalysts on single-atom alloys. *Chem. Sci.* **2021**, *12*, 10634-42. DOI PubMed PMC
46. Yang, S.; Si, Z.; Li, G.; et al. Single cobalt atoms immobilized on palladium-based nanosheets as 2D single-atom alloy for efficient hydrogen evolution reaction. *Small* **2023**, *19*, e2207651. DOI
47. Jin, R.; Li, G.; Sharma, S.; Li, Y.; Du, X. Toward active-site tailoring in heterogeneous catalysis by atomically precise metal nanoclusters with crystallographic structures. *Chem. Rev.* **2021**, *121*, 567-648. DOI
48. Walsh, A. G.; Zhang, P. Thiolate-protected single-atom alloy nanoclusters: correlation between electronic properties and catalytic activities. *Adv. Mater. Inter.* **2021**, *8*, 2001342. DOI
49. Kumar, B.; Kawawaki, T.; Shimizu, N.; et al. Gold nanoclusters as electrocatalysts: size, ligands, heteroatom doping, and charge dependences. *Nanoscale* **2020**, *12*, 9969-79. DOI
50. Kwak, K.; Choi, W.; Tang, Q.; et al. A molecule-like $PtAu_{24}(SC_6H_{13})_{18}$ nanocluster as an electrocatalyst for hydrogen production. *Nat. Commun.* **2017**, *8*, 14723. DOI PubMed PMC
51. Kwak, K.; Choi, W.; Tang, Q.; Jiang, D.; Lee, D. Rationally designed metal nanocluster for electrocatalytic hydrogen production from water. *J. Mater. Chem. A.* **2018**, *6*, 19495-501. DOI
52. Li, X.; Takano, S.; Tsukuda, T. Ligand effects on the hydrogen evolution reaction catalyzed by Au_{13} and $Pt@Au_{12}$: alkynyl vs thiolate. *J. Phys. Chem. C.* **2021**, *125*, 23226-30. DOI
53. Hu, G.; Tang, Q.; Lee, D.; Wu, Z.; Jiang, D. Metallic hydrogen in atomically precise gold nanoclusters. *Chem. Mater.* **2017**, *29*, 4840-7. DOI
54. Choi, W.; Hu, G.; Kwak, K.; et al. Effects of metal-doping on hydrogen evolution reaction catalyzed by MAu_{24} and M_2Au_{36} nanoclusters (M = Pt, Pd). *ACS. Appl. Mater. Interfaces.* **2018**, *10*, 44645-53. DOI
55. Jo, Y.; Choi, M.; Kim, M.; Yoo, J. S.; Choi, W.; Lee, D. Promotion of alkaline hydrogen production via Ni-doping of atomically precise Ag nanoclusters. *Bulletin. Korean. Chem. Soc.* **2021**, *42*, 1672-7. DOI
56. Ding, H.; Liu, H.; Chu, W.; Wu, C.; Xie, Y. Structural transformation of heterogeneous materials for electrocatalytic oxygen evolution reaction. *Chem. Rev.* **2021**, *121*, 13174-212. DOI PubMed
57. Luo, X.; Wei, X.; Zhong, H.; et al. Single-atom Ir-anchored 3D amorphous NiFe nanowire@nanosheets for boosted oxygen evolution reaction. *ACS. Appl. Mater. Interfaces.* **2020**, *12*, 3539-46. DOI
58. Babu, D. D.; Huang, Y.; Anandhababu, G.; et al. Atomic iridium@cobalt nanosheets for dinuclear tandem water oxidation. *J. Mater. Chem. A.* **2019**, *7*, 8376-83. DOI
59. Mu, X.; Yu, M.; Liu, X.; et al. High-entropy ultrathin amorphous metal–organic framework-stabilized Ru(Mo) dual-atom sites for water oxidation. *ACS. Energy. Lett.* **2024**, *9*, 5763-70. DOI

60. Su, L.; Wang, P.; Wang, J.; et al. Pt–Cu interaction induced construction of single Pt sites for synchronous electron capture and transfer in photocatalysis. *Adv. Funct. Mater.* **2021**, *31*, 2104343. DOI
61. Pan, Y.; Qian, Y.; Zheng, X.; et al. Precise fabrication of single-atom alloy co-catalyst with optimal charge state for enhanced photocatalysis. *Natl. Sci. Rev.* **2021**, *8*, nwaa224. DOI PubMed PMC
62. Du, X. L.; Wang, X. L.; Li, Y. H.; et al. Isolation of single Pt atoms in a silver cluster: forming highly efficient silver-based cocatalysts for photocatalytic hydrogen evolution. *Chem. Commun.* **2017**, *53*, 9402-5. DOI
63. Zhang, Y.; Chen, D.; Meng, W.; Li, S.; Meng, S. Plasmon-induced water splitting on Ag-alloyed Pt single-atom catalysts. *Front. Chem.* **2021**, *9*, 742794. DOI PubMed PMC
64. Kurashige, W.; Hayashi, R.; Wakamatsu, K.; et al. Atomic-level understanding of the effect of heteroatom doping of the cocatalyst on water-splitting activity in AuPd or AuPt alloy cluster-loaded $BaLa_4Ti_4O_{15}$. *ACS. Appl. Energy. Mater.* **2019**, *2*, 4175-87. DOI
65. Liu, Y.; Long, D.; Springer, A.; et al. Correlating heteroatoms doping, electronic structures, and photocatalytic activities of single-atom-doped $Ag_{25}(SR)_{18}$ nanoclusters. *Solar. RRL.* **2023**, *7*, 2201057. DOI